International Journal of Applied Pharmaceutics

ISSN- 0975-7058 Vol 12, Issue 2, 2020

Original Article

TOPICAL ANTI-PSORIATIC NANOPARTICULATE DRUG DELIVERY SYSTEM

KIRAN BHISE[1*], SHADAB KHAN[1], GHAZALA MULLA[2]

[1]Department of Pharmaceutics, M. C. E. Society's Allana College of Pharmacy, Pune, India, [2]Department of Physiology, Z. V. M. Unani Medical College and Hospital, Pune, India
Email: ksbhise@rediffmail.com

Received: 03 Dec 2019, Revised and Accepted: 29 Jan 2020

ABSTRACT

Objective: Development of effective drug delivery in the treatment of psoriasis is the major challenge for its successful management. To develop and assess the potential of Nanostructured Lipid Carriers (NLCs) enriched with the powdered leaves extracts of *Azadirachta indica* (AE), *Lawsonia inermis* (LE) and fruit extract of *Mallotus philippensis* (ME) in the management of psoriasis.

Methods: Drug loaded NLCs were prepared via hot homogenization technique by adopting 2^3 factorial design with factors X1 as the concentration of lipids, X2 concentration of surfactants and X3 being the number of homogenization cycle. The responses Y1 and Y2 were particle size and zeta potential. The optimized batch was obtained from Surface response plot and was evaluated for zeta potential, % entrapment efficiency, % drug loading, Scanning Electron Microscopy(SEM), % *in vitro* diffusion of drugs from the NLCs, anti-lipid peroxidation and nitric oxide scavenging activities, cytotoxicity on HaCat cell lines, Mouse Tail and Rat ultraviolet ray B photodermatitis models for Psoriasis.

Results: The optimized batch of NLCs was found within the nanosized range with a relatively low polydispersity index and zeta potential of-20mV. The %EE for an optimized batch of NLCs was found to be 98.97±0.83%, 96.99±0.56% and 99.25±0.55% and the %DL of 21.84±0.15%, 8.55±045%, and 87.91±0.38% respectively for AE, LE and ME.

The SEM images showed the spherical vesicular structures of drugs loaded NLCs. The *in-vitro* diffusion of drugs from the NLCs followed initial burst release thereafter sustained release for 24 h. The AE, LE and ME loaded NLCs proved to possess anti-lipid peroxidation and nitric oxide scavenging activities, cytotoxicity on HaCat cell lines, DNA fragmentation on HaCat cell lines which are biomarkers in the pathogenesis of psoriasis. The results of Mouse Tail and Rat ultraviolet ray B photodermatitis models for Psoriasis supported the anti-psoriatic potential of AE, LE and ME loaded NLCs.

Conclusion: AE, LE and ME loaded NLCs can be used for prolonged topical delivery to the psoriatic skin for an effective treatment.

Keywords: Psoriasis, Drug Extracts, Nanostructured Lipid Carriers, Evaluation

DOI: http://dx.doi.org/10.22159/ijap.2020v12i2.36536. Journal homepage: https://innovareacademics.in/journals/index.php/ijap

INTRODUCTION

Psoriasis is a common skin disease characterized by hyper-proliferation of epidermal cells of skin [1]. Although extensive work has been reported, the development of effective drug delivery is the major challenge for the successful management of this disease [2-27]. The barrier effect of skin offers several challenges for the topical bioavailability from conventional formulations. The literature review indicates the potential role of Nanostructured Lipid Carriers (NLCs) in the topical treatment of psoriasis [20-27]. Attempts to use topical allopathic treatments like corticosteroids, calcipotriene, retinoids, coal tar, anthralin, clobetasol propionate, methotrexate, cyclosporines have failed due to their toxicities and inappropriate formulation design of the conventional dosage forms [28-30]. The literature survey reveals that *Azadirachta indica, Lawsonia inermis,* and *Mallotus philippensis* exhibit anti-inflammatory activities in addition to their multitude of medicinal properties and have been used in combination in traditional medicine in the treatment of Psoriasis [31-35]. Different nanoparticulate drug delivery systems of *Azadirachta indica* have been reported in the literature such as Nanoemulsion, Nanocapsules, Solid lipid nanoparticles, and the Niosomes and Silver Nanoparticles of *Lawsonia inermis* leaves extract but no work has been done on nanoparticulate drug delivery system of *Mallotus philippensis* [36-40]. Also, the literature survey revealed the absence of *Azadirachta indica, Lawsonia inermis, and Mallotus philippensis* extracts loaded NLCs for the treatment of psoriasis. Therefore, the present research was undertaken to investigate and assess the potential of Nanostructured Lipid Carriers (NLCs) enriched with the powdered leaves extracts of *Azadirachta indica* (AE), *Lawsonia inermis* (LE) and fruit extract of *Mallotus philippensis* (ME) respectively. In this study the authors have investigated the long-term safety and efficacy of a three-compound formulation AE, LE and ME extract for the treatment of psoriasis.

MATERIALS AND METHODS

Materials

The Dried herbs of *Azadirachta indica* Leaves, *Lawsonia inermis* Leaves and *Mallotus philippensis* powder were purchased from local vendors and authenticated (Ref No.: Bot/10/2017) from the Department of Botany, Savitribai Phule University of Pune, India. The solid lipids were obtained as gift samples from Gattefosse, France. Rest all chemicals were of AR grade and were purchased from Sigma Aldrich.

Preparation of *Azadirachta indica* extract (AE), *Lawsonia inermis* extract (LE) and *Mallotus philippensis* extract (ME) loaded NLCs

The extracts were prepared from the leaves of *Azadirachta indica* and *Lawsonia inermis* using the Soxhlet apparatus and that of *Mallotus philippensis* fruits by maceration process and Drug loaded NLCs were produced by hot high-pressure homogenization method [41]. The factorial batches of AE, LE and ME loaded NLCs were prepared by applying 2^3Factorial Design [42] with factors, X1 (Stearic acid: Seasame oil, Mustard oil concentration), X2 (Tween80: Span 20 concentration) and X3 (number of homogenization cycle) as three independent variables at two levels–1 and+1. The two dependent responses were Y1 (Particle size) and Y2 (Zeta Potential). Accordingly, a total of eight formulations were designed and the compositions of different formulations have been depicted in table 1. The pre-emulsion was prepared by thoroughly dissolving the ME in the lipid phase containing stearic acid, sesame oil, mustard oil and span 20 at 65 °C, the oil phase was immediately dispersed into the hot aqueous phase consisting of Tween 80, AE and LE at 65 °C under constant stirring at 8000 rpm for 20 min using Ultra Turrax IKA T25, (Remi Motors Ltd, RM-12C Mumbai). For 2 gm of lipid mixture, 200 mg of AE, LE and ME mixture was taken in the ratio of 2.5:1:10. The pre-emulsion was further processed by high-pressure homogenizer

(Nitro Soavi, Italy) using 5 and 3 homogenization cycles (For factorial batches) at the temperature of 65 °C with 500bars pressure and cooled to room temperature so as to crystallize the lipid and finally formed the active-loaded NLCs.

Table 1: 2^3 Factorial batches

Factorial batch		Coded form			Actual form			AE, LE and ME (mg)
Sr. No.	NLC	X1	X2	X3	Conc. Of SA: SO and MO (g)	Conc. Of Tw80: Sp20 (g)	No. of Homogeni-zation cycles	
1.	F1	+	-	+	1.6	0.4	5	200
2.	F2	+	-	-	1.6	0.4	3	200
3.	F3	+	+	+	1.6	0.8	5	200
4.	F4	+	+	-	1.6	0.8	3	200
5.	F5	-	-	+	1.2	0.4	5	200
6.	F6	-	-	-	1.2	0.4	3	200
7.	F7	-	+	+	1.2	0.8	5	200
8.	F8	-	+	-	1.2	0.8	3	200

Physicochemical characterization of AE, LE and ME loaded NLC

Mean particle size, size distribution and charge on drug-loaded droplet surface of factorial batches of NLCs were determined by dynamic light scattering using Malvern Zetasizer at room temperature. Before measurement, batches were diluted with filtered double distilled water (1:1000) until the appropriate concentration of particles was achieved to avoid multi-scattering. The diluted samples were filled in the disposable transparent sizing cuvettes for measurement [43, 44].

Determination of drug entrapment efficiency (% EE)

AE, LE and ME entrapped within the NLCs were determined by centrifugation method. A volume of 10 ml of NLC dispersion was withdrawn and transferred to the Eppendorf tube. The unentrapped drug was separated from the NLCs by subjecting the dispersion to centrifugation in a cooling centrifuge (Remi Instrument Ltd, Mumbai) at 15000 rpm at a temperature of 4 °C for 60 min, whereupon the particles of NLCs and the supernatant containing the free drug were obtained. The supernatant was analyzed in triplicate for the drug content after suitable dilution with methanol by measuring absorbance at 214, 276 and 297 nm for AE, LE and ME using UV-VIS spectrophotometer [45].

The % entrapment efficiency was expressed as the percentage of total drug entrapped using the following formula:

$$\%\,EE = \frac{\text{Amount of drug entrapped in NLCs}}{\text{Theoretical amount of drug added to formulation}} \times 100$$

Determination of % drug loading (% DL)

For the determination of drug loading capacity, accurately weighed 5 mg of NLCs were dissolved in 5 ml of methanol and the solution was filtered through Whatman filter paper grade 41 to get recovered NLCs and the drug concentrations were determined using UV visible spectrophotometer at 214, 276 and 297 nm respectively for AE, LE and ME samples [46]. The percentage of drug loading capacity was determined using the following formula:

$$\%\ \text{Drug Loading} = \frac{\text{Mass of Drugs in NLCs}}{\text{Mass of NLCs recovered}} \times 100$$

***In vitro* % drug diffusion**

In vitro diffusion studies were performed using DBK diffusion cell apparatus and dialysis membrane-70 (PALL Corporation) with average diameter 17.5 mm and molecular weight cut-off between 12,000–14,000. Phosphate buffer pH-6.8: Methanol (7:3) was used as a diffusion medium. The dialysis membrane soaked for 12 h prior to the study with 50 mg of lyophilized NLCs was mounted on the Franz diffusion cells filled with 20 ml of diffusion media with constant stirring at 200rpm at 37 °C±0.5 °C. Accurately measured 1 ml of the sample was withdrawn at time intervals of one hour for 24 h maintaining the sink condition, followed by dilution with the Phosphate Buffer pH-6.8: Methanol (7:3) in the ratio 1:10. The samples were analyzed at a wavelength 214 nm, 276 and 297 nm for AE, LE and ME respectively using UV spectrophotometer (V-630, Jasco International, Tokyo, Japan). The cumulative % drug diffused for each drug in the NLC was determined graphically [47].

Scanning electron microscopy (SEM) of AE, LE and ME loaded NLC

SEM analysis of the AE, LE and ME loaded NLCs was carried by drop-casting method on a silicon wafer. A drop of NLC dispersion was used as a sample for SEM analysis. The sample was analyzed under the Scanning Electron Microscope (SEM, Nova Nano SEM) at an accelerating voltage of 20 kV [44, 47].

Lipid peroxidation assay

Lipid peroxidation was determined based on the amount of Thiobarbituric acid reactive substances. The HepG2 cells were seeded in 24-well culture plates at an initial density of $2*10^5$ cells/ml and grown to approximately 80% confluence. Oxidative stress was induced by treating the cells with freshly prepared H_2O_2. The cells were pretreated with samples (NLCs) at indicated concentrations for 24 h. Fetal Bovine Serum-free Dulbecco's Modified Eagle's medium containing H_2O_2 (882nM) was added to each well and the cell plate was incubated for 24 h. The HepG2cells were lysed by using the freeze-thaw method. After analysis, 0.2 ml of the cell suspension was added to the Thiobarituric acid reagent. This mixture was incubated at 90 °C for 1 h and then cooled. Four milliliters of a mixture of n-butanol and pyridine (15:1, v/v) was added and was centrifuged for15 min and the absorbance was measured at 532 nm [48, 49].

The percentage inhibition of lipid peroxidation was calculated using the following formula:

$$\%\ \text{inhibition} = \frac{\text{Absorbance (control)} - \text{Absorbance (test sample)}}{\text{Absorbance (control)}} \times 100$$

Nitric oxide scavenging assay

Accurately 200 µl of 10 mmol sodium nitroprusside and 200 µl of the test solution and reference standard of various concentrations were incubated at room temperature for 150 min. About 500 µl Griess reagent was added and was subjected to incubation for 10 min at room temperature. The absorbance was measured at 546 nm. Test substances were replaced by Phosphate buffer solution pH 7.0 for control [50].

The percentage inhibition of Nitric Oxide was calculated as follows:

$$\%\ \text{inhibition} = \frac{\text{Absorbance (control)} - \text{Absorbance (test sample)}}{\text{Absorbance (control)}} \times 100$$

Cytotoxicity studies on HaCat cell lines

HaCaT cell line was procured from ATCC, stock cells were cultured in Dulbecco's Modified Eagle's medium supplemented with 10% inactivated Fetal Bovine Serum, Penicillin (100 IU/ml), Streptomycin (100 µg/ml) in a humidified atmosphere of 5% Carbon dioxide at 37 °C. Serial two-fold dilutions (0-100µM) were prepared

for carrying out cytotoxic studies. The monolayer cell culture was trypsinized and the cell count was adjusted to 1.0 x 10^5 cells/ml using respective media containing 10% Fetal Bovine Serum. To each well of the 96 well microtiter plate, 100 µl of the diluted cell suspension (50,000 cells/well) was added. After 24 h, when a partial monolayer was formed, the supernatant was discarded, washed the monolayer once with medium and 100 µl of different test concentrations of NLCs was added on to the partial monolayer in microtiter plates followed by incubation at 37 °C for 24 h in 5% Carbon dioxide atmosphere. After incubation, the test solutions in the wells were discarded and 100 µl of 3-[4, 5-dimethylthiazol-2-yl]-2, 5-diphenyl tetrazolium bromide (5 mg/10 ml of MTT in USP Phosphate buffer pH 7.0) was added to each well. The plates were incubated for 4 h at 37 °C in a 5% Carbon dioxide atmosphere. The supernatant was removed and 100 µl of Dimethyl sulfoxide was added and the plates were gently shaken to solubilize the formed formazan. The absorbance was measured using a microplate reader at a wavelength of 590 nm. The percentage growth inhibition was calculated using the following formula and concentration of test drug needed to inhibit cell growth by 50% (IC_{50}) values were generated from the dose-response curves for each cell line [51, 52].

$$\% \text{ inhibition} = 100 - \frac{\text{OD of sample}}{\text{OD of control}} \times 100$$

DNA fragmentation studies on HaCat cell lines

HaCat cells were seeded at a concentration of 1x10^6 per 35 mm dish incubated at 37 °C/5 % Carbon dioxide for 24 h. The confluent cells grown after 24 h of incubation were treated with sample conc.160µg/ml, 320µg/ml and control. After treatment, cells were trypsinized, and both adherent and floating cells were collected by centrifugation at 2000 rpm for 5 min. The cell pellet was suspended in 0.5 ml lysis buffer pH 7.8 containing a mixture of Tris-Hydrochloric acid 10 mmol, pH 8; Ethylene diamine tetraacetic acid 20 mmol, pH 8.0; TritonX-100 0.2% or Sodium-*N*-lauroyl sarcosinate, 4M Sodium chloride, vortex vigorously and incubated at 50 °C for 5 min. To the lysate, 0.5 ml of phenol-chloroform iso-amyl alcohol was added and mixed for 2-3 min and centrifuged at 10000 rpm for 15 min at 4 °C. The upper aqueous layer was taken in a new tube, to which double the volume of cold 100% ethanol was added and 3M sodium acetate was added to make a final concentration of sodium acetate 0.3 M. The sample was incubated for 5-10 min at room temperature and centrifuged at 10000 rpm for 15 min. After removing the supernatant, the DNA pellets were washed with 70% ethanol and centrifuged at 5000 rpm for 10 min followed by removal of supernatant and air drying of DNA pellets that were dissolved in tris buffer and separated by 2% agarose gel electrophoresis at 100 volts for 50 min [53, 54].

Mouse-tail model for psoriasis

All procedures of the study were in accordance with the guidelines set by the CPCSEA and an approved IAEC protocol number (IAEC-17-019). 15 male Swiss albino Mice obtained from the National Institute of Bioscience, Pune were allowed to acclimatize for 5 d and randomly allotted to three groups, 6 mice per standard Group I, Clobetasol propionate 0.05% cream and NLCs Group II and 3 mice for placebo control Group III. The samples were applied to tails treated locally at the rate of 2-5 mg per animal to the proximal part of the tail uniformly. For the contact time of 2 h, a plastic cylinder was slipped over the tail and fixed with adhesive tape. At the end of contact time, the cylinders were removed and the tails were wiped with cotton. Mice were treated once daily, for 2 w. Two hours after the last treatment the animals were sacrificed and the tails were fixed in 10% buffered formalin and processed for histopathology. Longitudinal sections of about 5µm thickness were prepared and stained with hematoxylin-eosin and permanent slides were prepared for evaluation. Sections were examined under a light microscope to observe alterations in epidermal thickness, elongation of ridges and orthokeratosis. The animals were also observed for mortality and clinical sign and changes in body weights [55].

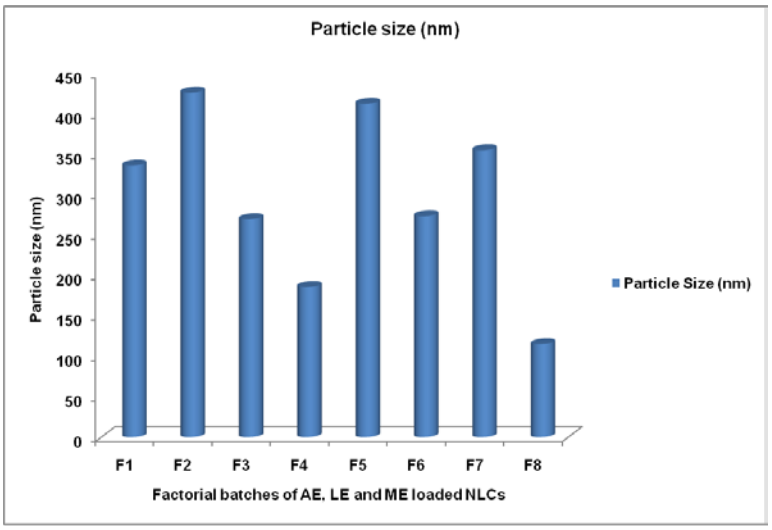

Fig. 1: Particle size analysis of factorial batches of AE, LE and ME loaded NLCs, Foot Note: (n=1) AE= *Azadirachta indica* extract, LE= *Lawsonia inermis* extract, ME= *Mallotus phillipensis* extract, NLCs= nanolipid carriers

Rat ultraviolet ray B photodermatitis model for psoriasis

Healthy male Sprague Dawley rats obtained from National Institute of Bioscience, Pune weighing 150-200 gm were kept in 12hour light: 12 hr dark cycle at 20.4 to 23.8 °C temperature and 36 to 61 % RH with the provision of food (*ad libitum*) and water (Reverse osmosis water treated with Ultraviolet light) were carefully maintained. All procedures of the study were in accordance with guidelines set by the CPCSEA and an approved IAEC protocol number (IAEC-17-009). The study design comprised of three groups, Group I (2-5 mg/kg of Clobetasol propionate 0.05% cream as standard) 6 animals, Group II (2-5 mg/kg of AE, LE and ME loaded NLCs) 6 animals and Group III (2-5 mg/kg of Placebo cream) 3 animals respectively. The hair on the dorsal skin was clipped and carefully shaved. An area (1.5 x 2.5 cm) on one side of the flank was irradiated for 15 min (1.5 J/cm2) at a vertical distance of 20 cm with UV-B LAMPS. Biphasic erythema was observed. After 72 h irradiation the test anti-psoriatic cream, standard cream, and placebo cream were applied at the 2-5 mg/rat topically on the irradiated site daily once. The irradiated rats were sacrificed on day 11 after UV-B irradiation by CO2 anesthesia. Skin biopsies were taken immediately, and fixed in 10% formalin and embedded in paraffin. Tissue sections (4 µm thick) were stained

with hematoxylin and eosin. Sections were examined under a light microscope to observe alterations in epidermal thickness, elongation of ridges and orthokeratosis. Parameters evaluated included mortality and clinical signs observations and body weight. All the data were analyzed using one way ANOVA followed by Dunnett's Multiple Comparison test [56, 57].

RESULTS AND DISCUSSION

Physicochemical characterization of factorial batches of AE, LE and ME loaded NLC

The dynamic light scattering method was employed for the determination of particle size and the charge on the surface of NLC droplets by using the Malvern Zetasizer (Hydro MU 2000, UK). The PDI values of the factorial batches of NLCs were obtained in a range of 0.453–1.01 with PDI of an optimized batch as 1, implying the polydispersity of NLCs. Zeta potential of-20 mV indicated good stability of colloidal dispersion. Average diameters, PDI and zeta potential of factorial batches of AE, LE and ME enriched NLCs have been shown in fig. 1.

Determination of %EE and %DL of factorial batches of AE, LE and ME loaded NLC

AE, LE and ME entrapped within the NLCs were determined by centrifugation method and were found to be in the range 98.65±0.06 to 99.07±0.09%, 94.58±0.31 to 95.91±0.09% and 98.79±0.24 to 99.08±0.58% respectively for AE, LE and ME as depicted in fig. 2 and the % drug loading of AE, LE and ME in NLC formulations ranged between 11.39±0.46 to 45.23±0.54%, 14.49±0.67-to45.23±0.37 and 40.85±0.89 to 86.24±0.74% respectively as depicted in fig. 3.

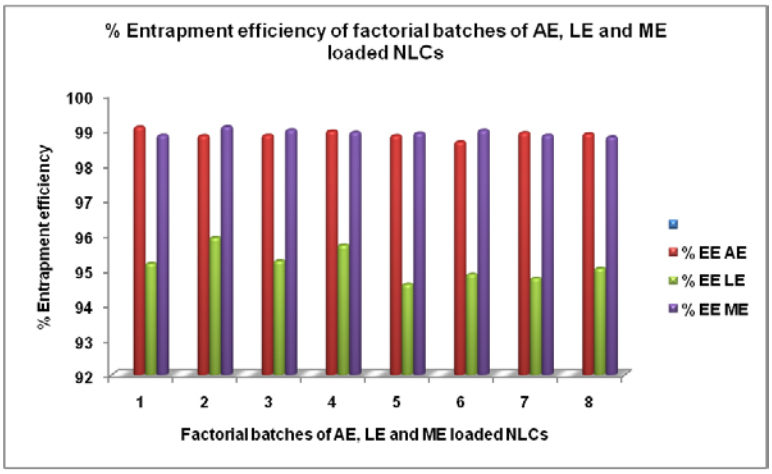

Fig. 2: % Entrapment efficiency of factorial batches of AE, LE and ME loaded NLCs, Foot Note: (n=3) all data representing an average of 3 trials, given as mean±SD, AE= Azadirachta indica extract, LE= Lawsonia inermis extract, ME= Mallotus phillipensis extract, NLCs= Nanolipid Carriers, %EE= percentage entrapment efficiency

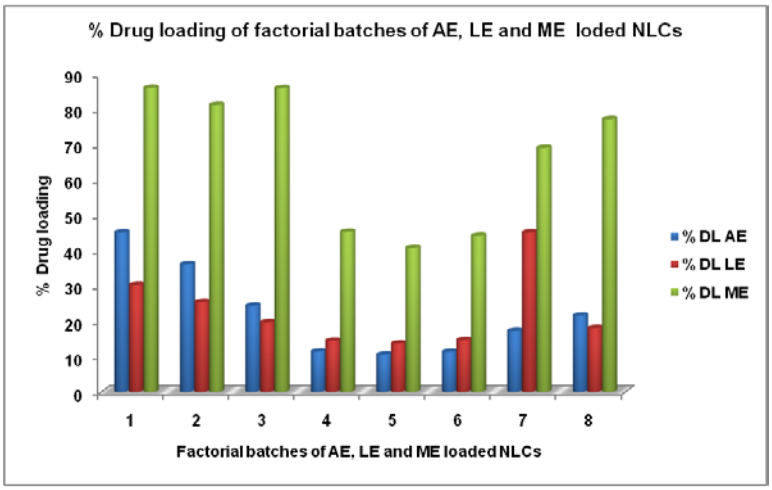

Fig. 3: % Drug loading of factorial batches of AE, LE and ME loaded NLCs, Foot Note: (n=3) all data representing an average of 3 trials, given as mean±SD, AE= *Azadirachta indica* extract, LE= *Lawsonia inermis* extract, ME= *Mallotus phillipensis* extract, NLCs= Nanolipid Carriers, %DL= percentage drug loading

In vitro % drug diffusion studies of factorial batches of AE, LE and ME loaded NLCs

In vitro % drug diffusion of factorial batches of AE, LE and ME loaded NLC was determined using franz diffusion cell apparatus that was found to range between 80.46±0.31 to 91.11±0.52%, 80.46±0.51 to 94.57±0.14% and 86.85±0.22 to 95.28±0.27% respectively at 24 h (fig. 4, 5 and 6). During the preparation of NLCs, cooling from high temperature to room temperature favors the enrichment of the drug in the outer layers of the particles resulting in superficial entrapment causing initial burst release.

Optimization of factorial batches of AE, LE and ME loaded NLC

A 2^3 randomized full factorial design was utilized in the present study. The different independent variables included Stearic Acid: Seasame oil and Mustard oil concentration (X1), Tween20: Tween80

concentration (X2) and Number of HPH cycles (X3). The batches were evaluated and the effect of an individual variable was studied according to the response surface methodology. The dependent response was Particle Size (Y). The three-dimensional (3D) response surface graphs depict the effect of the independent variables on the response (fig. 7).

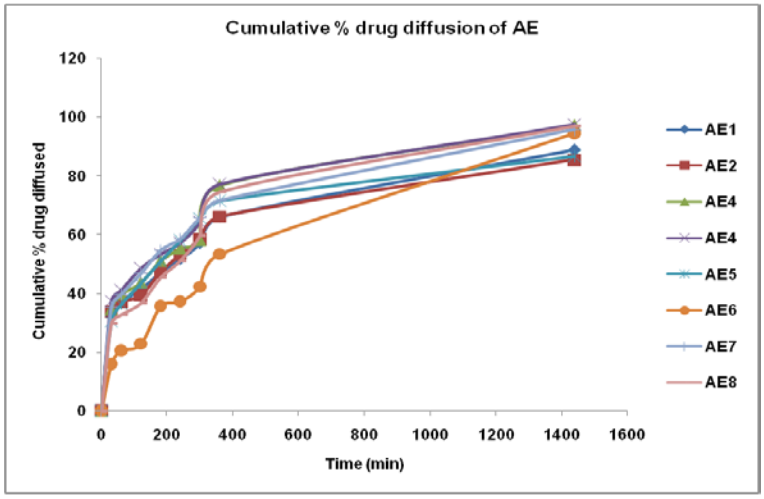

Fig. 4: Cumulative % drug diffusion of AE, footnote: (n=3) all data representing an average of 3 trials, given as mean±SD, AE= *Azadirachta indica* extract

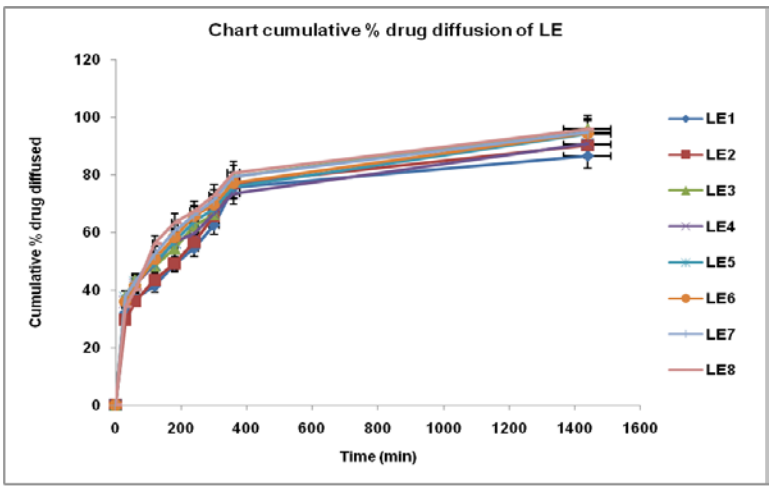

Fig. 5: Cumulative % drug diffusion of LE, Foot Note: (n=3) all data representing an average of 3 trials, given as mean±SD, LE= *Lawsonia inermis* extract

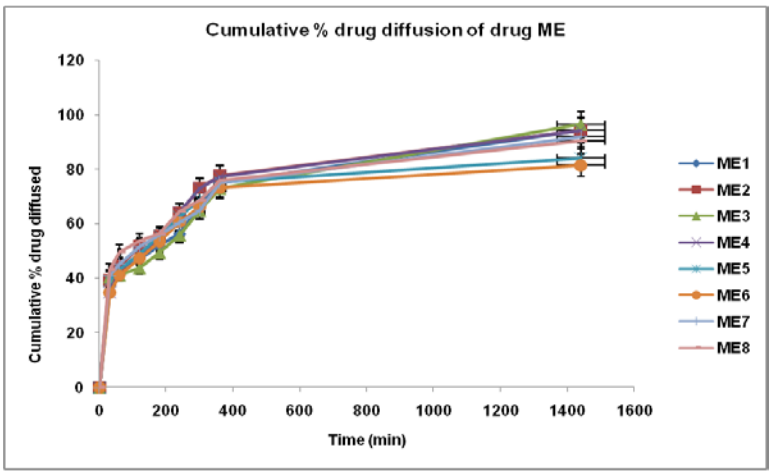

Fig. 6: Cumulative % drug diffusion of ME, Foot Note: (n=3) all data representing an average of 3 trials, given as mean±SD, ME= *Mallotus phillipensis* extract

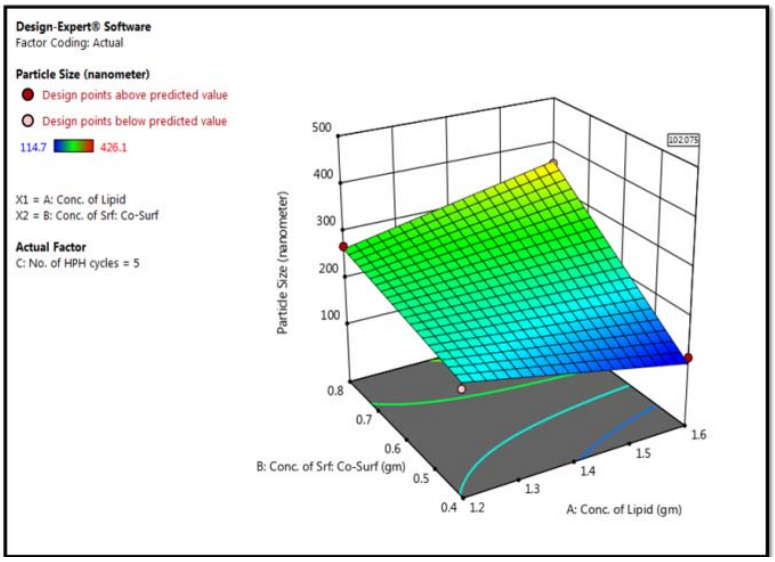

Fig. 7: Response surface plot (3D Surface Plot) showing the effect of formulation variables on particle size (Y1) of AE, LE and ME loaded NLCs

Physicochemical characterization of optimized batch of AE, LE and ME loaded NLC

The mean particle diameter/Z-average of the optimized batch of AE, LE and ME NLCs was found to be 185 nm Zeta potential of optimized formulation of AE, LE and ME loaded NLC was found to be-20 mV that indicates good stability of colloidal dispersion.

%EE and % DL of an optimized batch of NLCs

The %EE for the optimized batch of NLCs was found to be 98.97±0.83%, 96.99±0.56% and 99.25±0.55% and the %DL of 21.84±0.15%, 8.55±045%, and 87.91±0.38% respectively for AE, LE and ME with n=3.

Scanning electron microscopy (SEM) optimized batch

The SEM photomicrograph as indicated in fig. 8 reveals the spherical and smooth surface of the NLCs.

***In vitro* % drug diffusion of an optimized batch of AE, LE and ME loaded NLC**

As depicted in fig. 9 it was observed that % drug diffusion of AE, LE and ME was 90.87±4.71%, 92.64±1.56%, and 93.93±1.69 % respectively at 24th h.

Lipid peroxidation assay

Lipid peroxidation indicates the generation of malondialdehyde, increased levels of which play a significant role in the pathogenesis of Psoriasis [58]. The reduction in the levels of Malondialdehyde after application of AE, LE and ME loaded NLCs supported a reduction in inflammation and pathogenesis of psoriasis. As represented in fig. 10 the IC_{50} value of AE, LE and ME loaded NLCs for inhibition of lipid peroxidation was found to be 571.20 µg/ml confirming a dose-dependent increase in anti-lipid peroxidation.

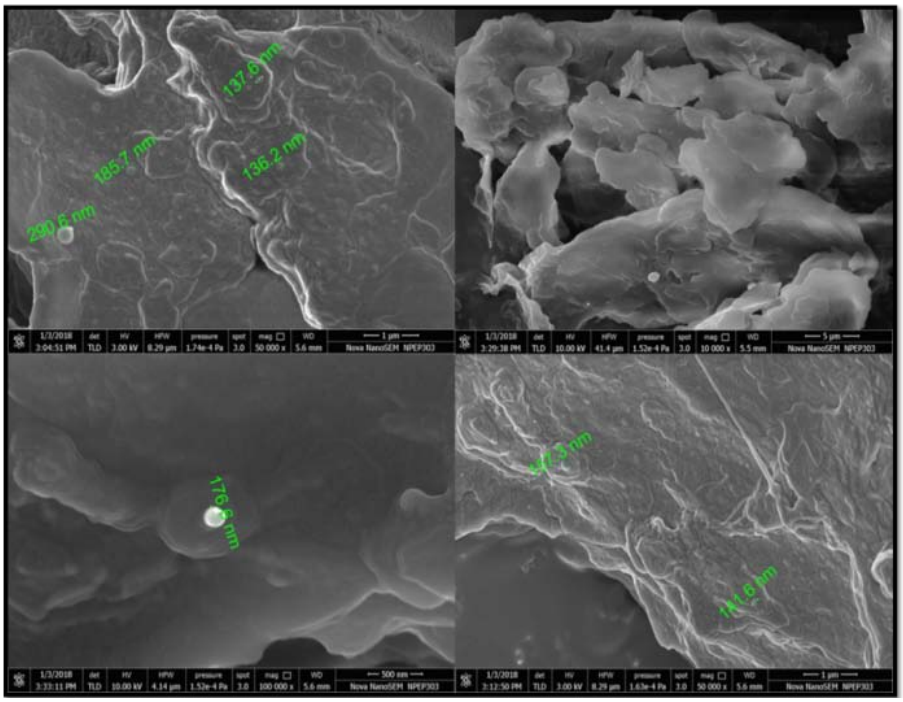

Fig. 8: Scanning electron microscopy of an optimized batch of AE, LE and ME loaded NLCs

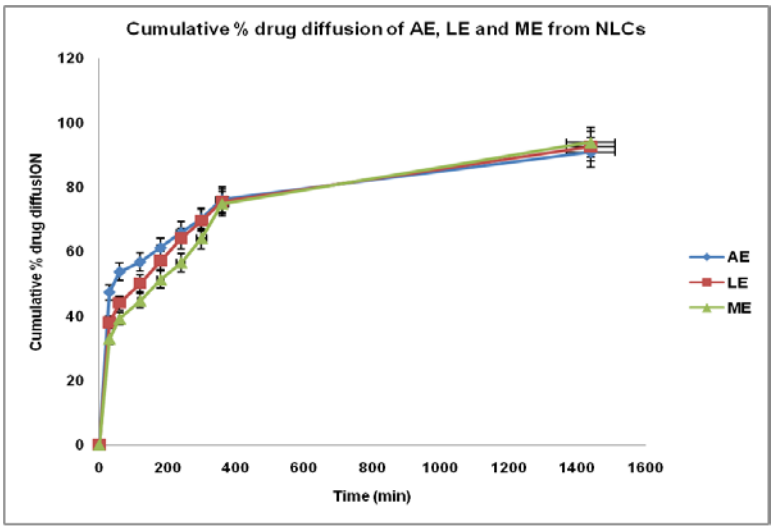

Fig. 9: ***In vitro*** **cumulative % drug diffusion for an optimized batch of AE, LE and ME loaded NLCs, Foot Note: (n=3) all data representing an average of 3 trials, given as mean±SD, AE=** ***Azadirachta indica*** **extract, LE=** ***Lawsonia inermis*** **extract, ME=** ***Mallotus phillipensis*** **extract, NLCs= nano lipid carriers**

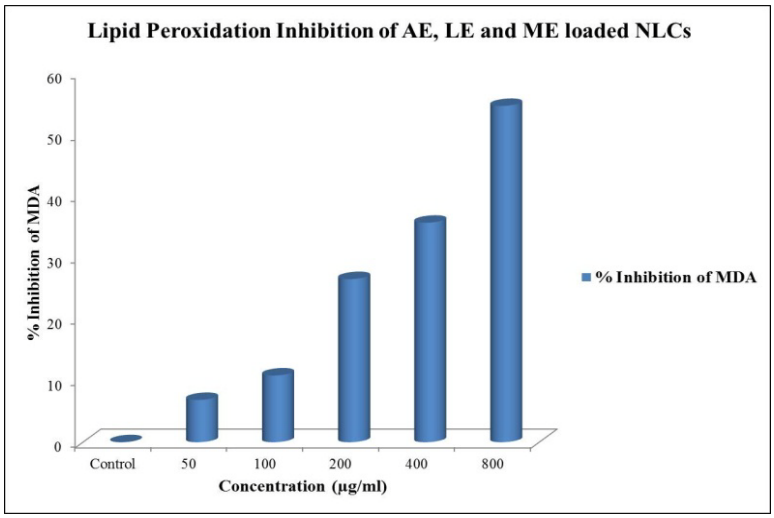

Fig. 10: Lipid peroxidation inhibition for optimized batch of AE, LE and ME loaded NLCs Foot Note: (n=1) AE= ***Azadirachta indica*** **extract, LE=** ***Lawsonia inermis*** **extract, ME=** ***Mallotus phillipensis*** **extract, NLCs= Nanolipid Carriers, MDA= Malondialdehyde**

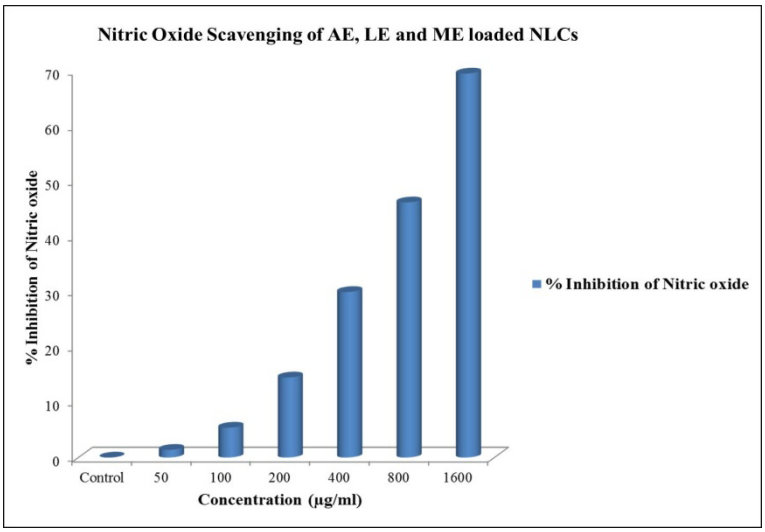

Fig. 11: % Nitric oxide inhibition for optimized batch of AE, LE and ME loaded NLCs, Foot Note: (n=1), AE= ***Azadirachta indica*** **extract, LE=** ***Lawsonia inermis*** **extract, ME=** ***Mallotus phillipensis*** **extract, NLCs= nanolipid carriers**

Nitric oxide scavenging assay

The nitric oxide scavenging activity was determined to assess peroxynitrite formation as it is an important factor in tissue-damaging mechanisms such as chronic inflammation [59]. The results presented in fig. 11 indicate the IC50 value of 899.79µg/ml suggesting the presence of nitric oxide scavenging activity in the NLCs.

Cytotoxicity studies

IC_{50} values for cytotoxicity test of AE, LE and ME loaded NLCs was derived from nonlinear regression analysis (curve fit) based on sigmoid dose-response curve (variable) and computed using Graph Pad Prism 6 (Graph pad, SanDiego, CA, USA) was found to be 164.2 µg/ml.

DNA fragmentation

HaCat cells treated with sample 160µg/ml, 320µg/ml have shown dose-dependent increased DNA fragmentation as compared with control. Overall, these results suggest that the sample induces DNA fragmentation; a marker of apoptotic activity in AE, LE and ME loaded NLCs.

Mousetail model for psoriasis

The objective of this Antipsoriatic activity study was to assess the orthokeratotic cell differentiation in the epidermal scales after the application of the formulation. No mortality or abnormal clinical signs or adverse effects of body weight gain were observed in any of the mice from the entire three groups until the scheduled necropsy.

Histopathology

Histopathological observations of the longitudinal sections of mouse tail skin from placebo Group III revealed the normal thickness of the epidermis, presence of ridges and presence of parakeratotic layer [fig. 12 (c)]. The mouse tail skin from standard Group I (Clobetasol propionate cream 0.05%) and test Group II (NLCs) groups revealed marked reduction in the thickness of the epidermal layer, a decrease in ridges and presence of granular cells in orthokeratotic layer [fig. 12 (a) and (b)] respectively.

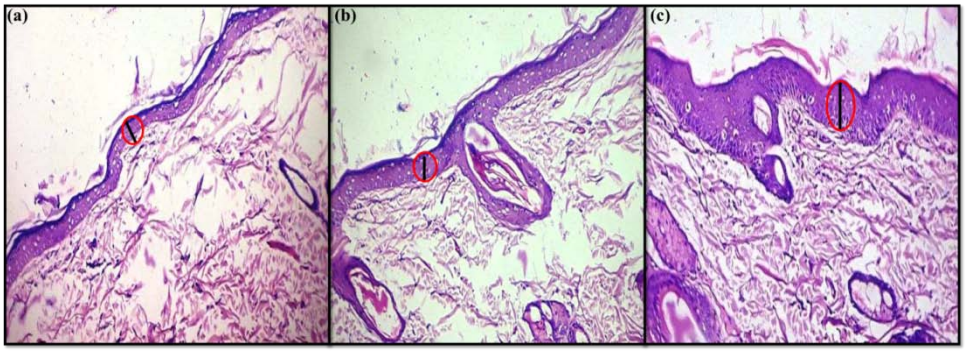

Fig. 12: Histopathology of mice tail skin for, a) Standard Group I, b) Test group II, c) Placebo group III

Rat ultraviolet ray B photodermatitis model for psoriasis

All the animals survived till the scheduled necropsy, there was no mortality or abnormal clinical signs of adverse effects on body weight gained of treated animals were observed in any animal throughout the treatment period. Animals were sacrificed on day 11 after induction of dermatitis and drug application. No gross pathological findings were observed in any of the control and treated animals.

Histopathology

Histopathological observations of the longitudinal sections of rat skin from placebo Group III revealed the increased thickness of epidermis with inflammatory changes [fig. 13 (c)]. The rat skin from standard Group I (Clobetasol propionate cream 0.05%) and test Group II (NLCs) groups revealed a marked reduction in the thickness of the epidermal layer and inflammatory changes [fig. 13 (a) and (b) respectively].

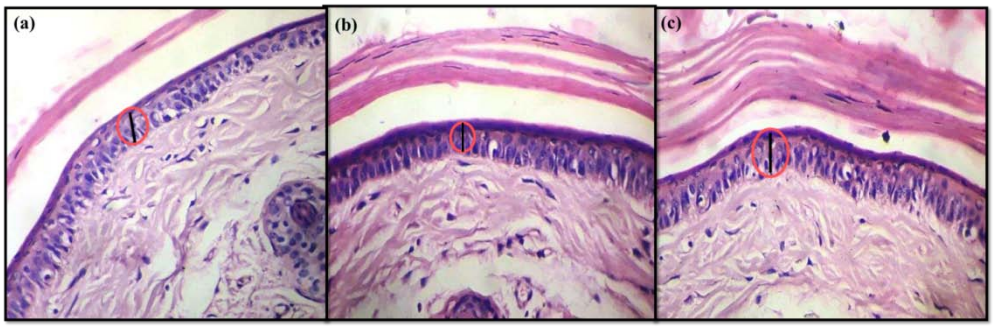

Fig. 13: Histopathology of Rat Skin for, a) Standard group I, b) Test group II, c) Placebo group III

FUTURE DIRECTION AND CONCLUSION

Nanotechnology is a growing field and is convincing to many researchers. Properly synthesized NLCs strategies result in the improvement of bioactivity and bioavailability of traditional herbs through encapsulation, particle size reduction, surfaces modification and bioactive materials entrapment for topical treatment of psoriasis. From the results of the cumulative drug diffusion studied, cell line studies and advanced preclinical trials of mouse tail and rat skin, it can be concluded that the AE, LE and ME loaded NLCs can be used for prolonged topical delivery of drugs to the psoriatic skin.

ACKNOWLEDGMENT

The authors wish to gratefully acknowledge the Ministry of AYUSH, Government of India, New Delhi, India for their generous funding support.

AUTHORS CONTRIBUTIONS

All the authors have contributed equally.

CONFLICT OF INTERESTS

Declared none

REFERENCES

1. Y Madhusudan Rao, Shayeda. Cosmeceuticals. PharmaMed Press; 2012. p. 194-253.
2. Magina S, Julia Vide. Moderate to severe psoriasis treatment challenges through the era of biological drugs. An Bras Dermatol 2017;92:668-74.
3. Chandrasekar R, Sivagami B. Alternative treatment for psoriasis-a review. Int J Res Dev Pharm L Sci 2016;5:2188–97.
4. Lowes MA, AM Bowcock, JG Krueger. Pathogenesis and therapy of psoriasis. Nature 2007;445:866-73.
5. Patricia M. Witman, topical therapies for localized psoriasis. Myo Clin Proc 2001;76:943-9.
6. Raza K, Singh B, Dogra S. Novel drug delivery systems in the topical treatment of psoriasis: rigors and vigors. Indian J Dermatol Venereol Leprol 2010;76:612-21.
7. Agarwal R, Katare OP, Vyas SP. Preparation and *in vitro* evaluation of liposomal/niosomal delivery systems for antipsoriatic drug dithranol. Int J Pharm 2001;228:43-52.
8. Ali MF, Salah M, Rafea M, Saleh N. Liposomal methotrexate hydrogel for the treatment of localized psoriasis: preparation, characterization and laser targeting. Med Sci Monit 2008;14:66-74.
9. Abdelbary AA, Abou Ghaly MH. Design and optimization of topical methotrexate loaded niosomes for enhanced management of psoriasis: Application of Box-Behnken design, *in vitro* evaluation, and *in vivo* skin deposition study. Int J Pharm 2015;485:235-43.
10. Trapasso E, Cosco D, Celia C, Fresta M, Paolino D. Retinoids: new use by innovative drug-delivery systems. Expert Opin Drug Delivery 2009;6:465-83.
11. Umalkar DG, Rajesh KS. Formulation and evaluation of liposomal gel for the treatment of psoriasis. Int J Pharma Bio Sci 2013;4:22-32.
12. Purushothamrao K, Khaliq K, Sagare P, Patil SK, Kharat SS, Alpana K. Formulation and evaluation of vanishing cream for scalp psoriasis. Int J PharmaSciTech 2010;4:32-31.
13. Su YH, Fang JY. Drug delivery and formulations for the topical treatment of psoriasis. Expert Opin Drug Delivery 2008;5:235-49.
14. Pradhan M, Singh D, Singh MR. Novel colloidal carriers for psoriasis: Current issues, mechanistic insight, and novel delivery approaches. J Controlled Release 2013;170:380-95.
15. Suresh PK, Singh P, Saraf S. Novel topical drug carriers as a tool for the treatment of psoriasis: progress and advances. Afr J Pharm Pharmacol 2013;7:138-47.
16. Dubey V, Mishra D, Dutta T, Nahar M, Saraf DK, Jain NK. Dermal and transdermal delivery of an anti-psoriatic agent via ethanolic liposomes. J Controlled Release 2007;123:148-54.
17. Zhang YT, Shen LN, Wu ZH, Zhao JH, Feng NP. Comparison of ethosomes and liposomes for skin delivery of psoralen for psoriasis therapy. Int J Pharm 2014;471:449-52.
18. Sah AK, Jain SK, Pandey RS. Microemulsion based hydrogel formulation of methoxsalen for the effective treatment of psoriasis. Asian J Pharm Clin Res 2011;4:140-5.
19. Behera J, Keservani RK, Yadav A, Tripathi M, Chadoker A. Methoxsalen loaded chitosan coated microemulsion for effective treatment of psoriasis. Int J Drug Delivery 2010; 2:159-67.
20. Lin YK, Huang ZR, Zhuo RZ, Fang JY. The combination of calcipotriol and methotrexate in nanostructured lipid carriers for topical delivery. Int J Nanomed 2010;5:117-28.
21. Lapteva M, Mondon K, Möller M, Gurny R, Kalia YN. Polymeric micelle nanocarriers for the cutaneous delivery of tacrolimus: a targeted approach for the treatment of psoriasis. Mol Pharm 2014;11:2989-3001.
22. Fang JY, Fang CL, Liu CH, Su YH. Lipid nanoparticles as vehicles for topical psoralen delivery: solid lipid nanoparticles (SLN) versus nanostructured lipid carriers (NLC). Eur J Pharm Biopharm 2008;70:633-40.
23. Pople PV, Singh KK. Development and evaluation of colloidal modified nano lipid carrier: application to topical delivery of tacrolimus, Part II–*in vivo* assessment, drug targeting, efficacy, and safety in treatment for atopic dermatitis. Eur J Pharm Biopharm 2013;84:72-83.
24. Pinto MF, Moura CC, Nunes C, Segundo MA, Costa Lima SA, Reis S. A new topical formulation for psoriasis: development of methotrexate-loaded nanostructured lipid carriers. Int J Pharm 2014;477:519-26.
25. Raza K, Singh B, Lohan S, Sharma G, Negi P, Yachha Y. Nano-lipoidal carriers of tretinoin with enhanced percutaneous absorption, photostability, biocompatibility, and anti-psoriatic activity. Int J Pharm 2013;456:65-72.
26. Surya Tej KVM, Moin A, Gowda DV, Anjali, Karunakar G, Patel NP. Nanostructured lipid carrier-based drug delivery system. J Chem Pharm Res 2016;8:627–43.
27. Gungor S, Rezigue M. Nanocarriers mediated topical drug delivery for psoriasis treatment. Curr Drug Metab 2017;18:454-68.
28. Gazi Shaikh, Sadath Ali, SY Talmale, Ulhas S Surwase, Kadam Bhalchandra, Shaikh Luqman. Alternative medicine for psoriasis–natural herbal ayurvedic treatment-a review. Int J Ayurvedic Herbal Med 2012;2:455–63.
29. Kaur T. Formulation development of anti-psoriatic topical babchi oil emulgel formulation development of anti-psoriatic topical babchi oil emulgel. Res Rev: J Herbal Sci 2017;2:1-14.
30. Chandrasekar R, Sivagami B. Alternative treatment for psoriasis-a review. Int J Res Dev Pharm Life Sci 2016;5:2188–97.
31. Naik MR, Bhattacharya A, Behera R, Agrawal D, Dehury S, Kumar S. Study of the anti-inflammatory effect of Azadirachta indica seed oil (Azadirachta indica) on infected albino rats. J Herbal Res Rev 2014;1:66–9.
32. Wiem A, Smail A, Wissem M, Faleiro M, Miguel M. Antioxidant, anti-inflammatory and anti-acetylcholinesterase activities of leaf, flower, and seed aqueous extracts of lawsonia inermis from tunisia. Int J Pharm Pharm Sci 2014;6:445–52.
33. Annavarapu T Rao, Renuka P, Akhil P, Divya P, P DP. Evaluation of the anti-inflammatory activity of combination of ethanol extracts of azadirachta Indica (Azadirachta indica) and lawsonia inermis (Lawsonia inermis). Asian J Pharm Clin Res 2016;9:9–11.
34. Gangwar M, Gautam MK, Ghildiyal S, Nath G, Goel RK. Pharmacological evaluation of mallotus philippinensis (Lam.) muell. Arg. fruit hair extract for anti-inflammatory, analgesic and hypnotic activity. J Intercult Ethnopharmacol 2016;5:14–21.
35. Ghazanavi, Khaklid. Amraz-e-Jildaur Ilaj-e-Nabvi. Farid Book Pvt Ltd; 2004. p. 123-136, 214-217, 257, 276.
36. Jayakumar Jerobin, Pooja Makwana, RS Suresh Kumar, Rajiv Sundaramoorthy, Amitava Mukherjee, Natarajan Chandrasekaran. Antibacterial activity of neem nanoemulsion and its toxicity assessment on human lymphocytes *in vitro*. Int J Nanomed 2015;10:77-86.
37. V Vijayan, Shaik Aafreen, S Sakthivel, K Ravindra Reddy. Formulation and characterization of solid lipid nanoparticles loaded Neem oil for topical treatment of acne. J Acute Disease 2013;2:282-6.
38. Tatiane Pasquoto Stigliani, Estefânia VR Campos, Jhones L Oliveira, Camila MG Silva, Natalia Bilesky Jose, Mariana Guilger, *et al*. Nanocapsules containing neem (Azadirachta Indica) oil: development, characterization, and toxicity evaluation. Sci Reports 2017;7:1-12.
39. SCG Kiruba Daniel, N Mahalakshmib, J Sandhiya, Kasi Nehru, Muthusamy Sivakumar. Rapid synthesis of Ag nanoparticles using henna extract for the fabrication of photoabsorption enhanced dye-sensitized solar cell (PEDSSC). Adv Materials Res 2013;678:349-60.
40. Mahmood Barani, Mohammad Mirzaei, Masoud Torkzadeh Mahani, Mohammad Hadi Nematollahi. Lawsone-loaded niosome and its antitumor activity in MCF-7 breast cancer cell line: a nano-herbal treatment for cancer. DARU J Pharm Sci 2018;26:11–7.

41. Qiang Xia, Hongxia Wang. Preparation and characterization of co-enzyme Q10 loaded nanostructured lipid carriers as delivery system for cosmetic component. NSTI-Nanotech 2010;3:498-501.
42. Banker GS, Rhodes CT. Modern pharmaceutics. 3rd edition. Optimization techniques in pharmaceutical formulation and processing. Marcel Dekker; 1996. p. 607.
43. Uprit S, Kumar Sahu R, Roy A, Pare A. Preparation and characterization of minoxidil loaded nanostructured lipid carrier gel for effective treatment of alopecia. Saudi Pharm J 2013;21:379–85.
44. Fouad EA, Yassin AEB, Alajami HN. Characterization of celecoxib-loaded solid lipid nanoparticles formulated with tristearin and softisan 100. Trop J Pharm Res 2015;14:205–10.
45. Souto EB, Wissing SA, Barbosa CM, Müller RH. Development of a controlled release formulation based on SLN and NLC for topical clotrimazole delivery. Int J Pharm 2004;278:71–7.
46. Chander Prakash Dora, Shailendra Kumar Singh, Sanjeev Kumar. Development and characterization of nanoparticles of glibenclamide by solvent displacement method. Acta Poloniae Pharm Drug Res 2010;67:283-90.
47. Gaba B, Fazil M, Khan S, Ali A, Baboota S, Ali J. Nanostructured lipid carrier system for topical delivery of terbinafine hydrochloride. Bull Fac Pharm Cairo Univ 2015;53:147–59.
48. Ohkawa H, Ohishi N, Yagi K. Assay for lipid peroxides in animal tissues by thiobarbituric acid reaction. Anal Biochem 1979; 95:351-8.
49. Panasenko OM, Evgina SA, Driomina ES. Hypochlorite induces lipid peroxidation in blood lipoproteins and phospholipid liposomes. Free Radical Biol Med 1995;19:133-40.
50. Yokozawa T, Wang ST, Chen PC, Hattori M. Inhibition of nitric oxide release by an aqueous extract of tinospora tuberculata. Phytother Res 2000;14:51-3.
51. T Mosmann. Rapid colorimetric assay for cellular growth and survival: application to proliferation and cytotoxicity assays. J Immunol Methods 1983;65:12-6.
52. Colombo I, Sangiovanni E, Maggio R, Mattozzi C, Zava S, Corbett Y, *et al.* HaCaT cells as a reliable *in vitro* differentiation model to dissect the inflammatory/repair response of human keratinocytes. Mediators of Inflammation 2017:1–12. Doi:10.1155/ 2017/ 7435621.
53. Li Z, Yu J, Liu L, Wei Z, Ehrlich ES. Coxsackie virus A16 infection induces neural cell and non-neural cell apoptosis *in vitro*. PLOS One 2014;9:1-10.
54. Takada M, Noguchi A, Sayama Y, Kurohane Kaneko Y, Ishikawa T. Inositol 1,4,5-trisphosphate receptor-mediated initial Ca(2+) mobilization constitutes a triggering signal for hydrogen peroxide-induced apoptosis in INS-1 β-cells. Biol Pharm Bull 2011;34:954-8.
55. Singhal M, Kansara N. Cassia tora linn cream inhibits psoriasis in mouse tail model. Pharm Crops 2012;3:1-6.
56. Manmohan Singhaland Niraj Kansara. *Cassia tora* linn cream inhibits ultraviolet-b-induced psoriasis in rats. ISRN Dermatol 2012;16:6.
57. Nakaguma H, Kambara T, Yamamoto T. Rat ultraviolet ray B photodermatitis: an experimental model of psoriasis vulgaris. Int J Exp Pathol 1995;76:65–73.
58. Nagamani M, Prahaladu P, Vijayababu PVSS, Ashalata K, Kusuma Kumari P, Kumari KL. Lipid peroxidation product as a marker of oxidative stress in psoriasis-a case-control study in north coastal Andhra Pradesh. IOSR J Dent Med Sci Ver II 2015;14:2279–861.
59. Ignacio NRS, Ferreira PLJ, Almeida BM, Kubelka FC. Nitric oxide production by murine peritoneal macrophages *in vitro* and *in vivo* treated with *Phyllanthus tenellus* extracts. J Ethnopharmacol 2001;74:181-7.
60. Shantanu Kuchekar, Kiran Bhise. Formulation and development of antipsoriatic herbal gel-cream. J Sci Industrial Res 2012;71:279-84.
61. Rajan A. Case study on beta-blockers induced psoriasis. Int J Pharm Pharm Sci 2019;11:112-5.
62. Pai G, N Sashidharan. Biologic armamentarium in psoriasis. Asian J Pharm Clin Res 2006;9:65-72.